Characterization of soluble iron in urban aerosols using near-real time data

Michelle Oakes,[1] Neeraj Rastogi,[1] Brian J. Majestic,[2] Martin Shafer,[3] James J. Schauer,[3] Eric S. Edgerton,[4] and Rodney J. Weber[1]

Received 22 May 2009; revised 30 November 2009; accepted 6 January 2010; published 5 August 2010.

[1] We present the first near-real time (12 min) measurements of fine particle (PM2.5) water soluble ferrous iron (WS_Fe(II)) measured in two urban settings: Dearborn, Michigan and Atlanta, Georgia. A new approach was used to measure WS_Fe(II) involving a Particle-into-Liquid Sampler (PILS) coupled to a liquid waveguide capillary cell (LWCC) and UV/VIS spectrometer. We found no clear diurnal trends in WS_Fe(II) at any urban site studied. High temporal variability, however, was observed at all urban sites, where concentrations often changed from the method limit of detection (4.6 ng m^{-3}) to approximately 300 to 400 ng m^{-3}, lasting only a few hours. These transient events predominately occurred during times of low wind speeds and appeared to be from local sources or processes. In Atlanta, several WS_Fe(II) events were associated with sulfate plumes, and highest WS_Fe(II) concentrations were found in plumes of highest apparent aerosol acidity. At all locations studied, WS_Fe(II) was poorly correlated ($R^2 < 0.34$) with light-absorbing aerosol, indicating no direct linkage between mobile source emissions and enhanced WS_Fe(II) concentrations. WS_Fe(II) measured within a prescribed forest-burn was strongly correlated with water soluble potassium ($R^2 = 0.88$; WS_Fe(II)/WS_K = 15 mg/g), pointing to biomass burning as a source of WS_Fe(II); however, peak concentrations within the fire were low compared to transient events observed at the urban sites. Overall, WS_Fe(II) temporal trends for these urban sites consisted of low background concentrations with periodic short duration transient events that appear to be linked to unique industrial emissions or atmospheric processing of industrial emissions that form WS_Fe(II).

Citation: Oakes, M., N. Rastogi, B. J. Majestic, M. Shafer, J. J. Schauer, E. S. Edgerton, and R. J. Weber (2010), Characterization of soluble iron in urban aerosols using near-real time data, *J. Geophys. Res.*, *115*, D15302, doi:10.1029/2009JD012532.

1. Introduction

[2] Iron is one of the most abundant transition metals in atmospheric aerosols that exists in a variety of chemical forms. As a redox–active metal, iron may be present in the oxidation states Fe(II) and Fe(III) and can cycle between these states through atmospheric processes that alter the aerosol composition [*Pehkonen et al.*, 1993]. The redox state of iron affects its reactivity and solubility, properties that determine environmental impacts, such as toxicity when inhaled and bioavailability to ecosystems [*Prahalad et al.*, 2001; *Shaked et al.*, 2005].

[3] Particulate iron catalyzes reactions through Fenton-like chemistry that produces reactive oxygen species (ROS), including hydrogen peroxide, the hydroxyl radical, and oxidized organic species [*Tao et al.*, 2003; *Vidrio et al.*, 2008; *Zhang et al.*, 2008]. Oxidative stress, triggered by toxic levels of ROS, is thought to be one cause of adverse health effects associated with aerosols due to mechanisms such as DNA strand breakage and tissue or cell damage [*Kelly*, 2003]. Several studies reported that the soluble iron fraction is more strongly correlated with ROS formation than the insoluble iron fraction in aerosol particles [*Prahalad et al.*, 2001; *See et al.*, 2007; *Valavanidas et al.*, 2000]. In addition, the oxidizing capacity of the atmosphere is also influenced by iron. Oxidation of atmospheric S(IV) to S(VI) by O_2 is catalyzed by transition-metals (Fe and Mn) [*Brandt and van Eldik.*, 1995, and references therein]. Recently, *Alexander et al.* [2009] estimated that metal-catalyzed (Fe and Mn) S(IV) oxidation by O_2 contributes between 9% and 17% of the global atmospheric sulfate pool. Iron also plays an important role in the global carbon cycle through effects on marine productivity. Deposition of aerosol particulate iron is thought to be a major source of soluble (bioavailable) iron to the open ocean that is a critical micronutrient for phytoplankton met-

[1]School of Earth and Atmospheric Sciences, Georgia Institute of Technology, Atlanta, Georgia, USA.
[2]Department of Chemistry and Biochemistry, Northern Arizona University, Flagstaff, Arizona, USA.
[3]Department of Civil and Environmental Engineering, University of Wisconsin-Madison, Madison, Wisconsin, USA.
[4]Atmospheric Research and Analysis, Inc., Durham, North Carolina, USA.

0148-0227/10/2009JD012532

abolic processes [*Gao et al.*, 2003; *Jickells et al.*, 2005; *Lam and Bishop*, 2008].

[4] Several studies have reported measurements of particulate iron in remote marine environments to characterize sources and assess the influence of iron on environmental systems. Sources include mineral dust from arid regions [*Claquin et al.*, 1999; *Journet et al.*, 2008], anthropogenic emissions [*Chuang et al.*, 2005; *Sedwick et al.*, 2007], and biomass burning emissions [*Guieu et al.*, 2005]. Of the total iron in ambient particles, the labile fraction available for biological processes is generally a small fraction, typically less than 1% to 10% in marine regions. However, this fraction can vary from less than 1% to nearly 50% depending upon proximity to sources and time of day or year [*Chen and Siefert*, 2004; *Johansen et al.*, 2000; *Zhu et al.*, 1993; *Zhuang et al.*, 1992]. In Barbados, *Zhu et al.* [1993] reported a day/night pattern, showing an average daytime labile Fe(II) concentration of 3.7 ng m^{-3} that was significantly higher than nighttime concentrations of 1.5 ng m^{-3} in total suspended particulates (TSP). Combined fine (particle diameter, D_p < 3 μm) and coarse (D_p > 3 μm) labile Fe(II) concentrations within the marine atmosphere during the Indian Ocean intermonsoonal period ranged from less than 0.4 ng m^{-3} to 4.75 ng m^{-3}, in contrast to concentrations below the detection limit (<0.34 to < 0.089 ng m^{-3}) during the southwest monsoonal season over the Arabian seas [*Siefert et al.*, 1999]. *Johansen et al.* [2000] reported a combined fine (D_p < 3 μm) and coarse (D_p > 3 μm) labile Fe(II) concentration of 3.14 ng m^{-3} in the North Atlantic marine atmosphere with a majority (86%) of the Fe(II) in the fine mode. A few recent studies have explored labile fractions of iron in urban environments. *Majestic et al.* [2006] found a mean soluble PM10 Fe(II) concentration of 19.6 ng m^{-3} in ambient samples from East St. Louis, Illinois. *Chuang et al.* [2005] recorded a mean soluble TSP Fe concentration of 32 ± 19 ng m^{-3} at Cheju, Korea.

[5] A variety of atmospheric processes can influence aerosol iron speciation and water solubility. Photochemistry and changes in particle pH are thought to be important mechanisms. Several studies have documented that Fe(III) photoreduction in the presence of organic compounds is an important source of Fe(II) in cloud and fog water [*Erel et al.*, 1993; *Faust and Hoigne*, 1988; *Faust and Zepp*, 1993; *Pehkonen et al.*, 1993; *Siefert et al.*, 1994]. More recent studies suggested that transformation of mineral dust to more labile forms of iron may occur via aerosol acidification involving urban pollutants [*Meskhidze et al.*, 2003; *Solmon et al.*, 2009].

[6] Atmospheric concentrations of water soluble Fe(II), hereafter denoted as WS_Fe(II), have been predominately measured by filtration techniques, where ambient aerosols are collected on filters over extended periods of time and then extracted into aqueous solution for subsequent analyses. The relatively long sample integration periods inherent with this method, typically 12 to 24 h, inhibits investigating variability in WS_Fe(II) concentrations over shorter time scales. Sample alteration during collection and analysis is also a potential drawback of filter-based methods. Interconversions of Fe(II)/Fe(III) on the filter during sample collection, sample storage, or the extraction process prior to analysis may result in measurement biases [*Majestic et al.*, 2006]. More highly time-resolved measurements have been shown to provide new insights into Fe sources [*Kidwell and Ondov*, 2004] and may also improve our understanding of chemical processes that alter iron's redox state.

[7] This study presents the first near-real time and continuous measurements of WS_Fe(II) (focusing mainly on PM2.5) made at a number of urban sites in the eastern United States: Atlanta, Georgia; Dearborn, Michigan; and a prescribed burn in Ichauway, Georgia. These results are compared with meteorology parameters and other highly time-resolved measurements of atmospheric species to characterize WS_Fe(II) temporal variability in order to investigate sources and atmospheric processes that may affect ambient WS_Fe(II) concentrations.

2. Methods

2.1. Instrument for Online Sampling

[8] Concentrations of WS_Fe(II) in ambient aerosols were measured continuously using a Particle-into-Liquid-Sampler (PILS) coupled to a portable ultraviolet visible light spectrometer (UV/VIS) (Ocean Optics, Dunedin, Florida, USA). Detection of WS_Fe(II) was based on the ferrozine technique of *Stookey* [1970]. To provide sufficient sensitivity, a liquid waveguide capillary flow-through optical cell (LWCC, World Precision Instruments, Sarasota, Florida, USA) with a long path length (100 cm) was utilized to measure optical (VIS) absorption of the ferrozine-iron complex. This fully automated method, hereafter referred to as the PILS-LWCC, provides 12 min integral WS_Fe(II) measurements in aerosols with a limit of detection (LOD) of 4.6 ng m^{-3} and analytical uncertainty of ~12%. The instrument was mainly used to measure WS_Fe(II) in particles smaller than 2.5 μm aerodynamic diameter by employing a PM2.5 cyclone inlet (URG, Chapel Hill, North Carolina, USA). For one sampling period (Atlanta, Georgia: November/December 2007), the size-selective inlet was removed to measure total WS_Fe(II), where the upper size limit (50% efficiency) is estimated to be approximately 10 μm diameter (denoted here as PM10). The upper size cutoff is determined by the transport efficiency of particles to the PILS (losses mainly due to settling) and PILS collection efficiency [*Orsini et al.*, 2003]. In the PILS-LWCC, the PILS system transfers particles to purified water, which is collected in a polypropylene vial. After 12 min of accumulation, the sample is pumped from the collection vial, combined with ferrozine, and directed through several mixing coils followed by the LWCC. The absorbance at 562 nm (maximum absorbance of WS_Fe(II)-ferrozine complex) and 700 nm (nonabsorbing reference wavelength) is measured. A four-point calibration using ammonium iron(II) sulfate acidified to pH 1 (typical R^2 = 0.9999) was used to determine the WS_Fe(II) concentration and was performed before and after each field study. A WS_Fe(II) standard was analyzed through the mixing system every week to check the precision of the calibration curve. During field studies, dynamic blank measurements were performed once or twice per day for 1–1.5 h duration to quantify any sample background, interferences, or other sampling artifacts. Mean blank concentrations were subtracted from the data to quantify ambient WS_Fe(II) concentrations. *Rastogi et al.* [2009] provides a detailed description of the PILS-LWCC and a comparison between the PILS-LWCC method and an integrated filter collection technique. Although the PILS-LWCC method marks significant improvement from filter-based methods in

terms of characterizing WS_Fe(II) temporal variability and identifying sources/sinks, a system capable of simultaneous WS_Fe(III) measurements would provide much greater insight into sources and atmospheric processes that influence water soluble iron concentrations.

2.2. The Sampling Sites

[9] Ambient concentrations of WS_Fe(II) from studies in Dearborn, Michigan; Atlanta, Georgia; and a prescribed burn of a forest under-story biomass (Ichauway, Georgia) are presented in this paper. The following section includes a short description of each sampling site and additional instrumentation used for measuring atmospheric components and parameters used in the WS_Fe(II) data interpretation.

2.2.1. Urban Studies: Dearborn, Michigan

[10] The PILS-LWCC with a PM2.5 inlet was deployed at a public school parking lot in Dearborn, Michigan (42.307°N, −83.150°W), a suburb ~20 km southwest of central Detroit, during the Lake Michigan Air Directors Consortium (LADCO) winter field campaign from 19 January to 8 February 2008. Detroit, Michigan, and its surrounding counties are consistently nonattainment areas for PM2.5 National Ambient Air Quality Standards. *Hammond et al.* [2008] have shown that air quality in east and southwest Detroit (near Dearborn, Michigan) is impacted by coal combustion, gasoline/diesel traffic, and industrial sources (iron/steel manufacturing plants, oil refineries, sewage sludge incinerator, and automotive manufacturing plants).

[11] The Dearborn sampling site was located in the center of the River Rouge industrial area, where many point sources, including power plants, steel mills, petroleum refineries, and auto plants, are located within a 10 km radius, and mixed with residential neighborhoods. A rail-switching yard directly south of the site and a steel mill that manufactures hot-rolled carbon steel sheet metal was approximately 1 km southwest of the site. Significant heavy-duty diesel truck traffic associated with industrial activity was common on local streets.

[12] Supporting measurements taken at this site included hourly concentrations of elemental and organic carbon (EC and OC) using an on-time OC-EC analyzer (Sunset Laboratory, Forest Grove, Oregon) following the NIOSH 5040 method. Hourly PM2.5 mass concentrations were measured with a Tapered Element Oscillating Microbalance (Thermo Fisher Scientific Inc., Waltham, Massachusetts). Hourly averaged meteorological data were available from a local meteorological station approximately 1km northwest of the sampling site.

2.2.2. Urban Studies: Atlanta, Georgia

[13] To provide insight on seasonal variability, the PILS-LWCC was deployed in Atlanta, Georgia, during periods in fall (PM10), spring (PM2.5), and summer (PM2.5) at two different sites: Fire Station 8 (33.802°N, −84.435°W) and Jefferson Street (33.776°N, −84.413°W). These sites are located approximately 3–4 km from central Atlanta and are separated by approximately 2 km. WS_Fe(II) measurements from these sites offer a general representation of the air quality in metropolitan Atlanta, although the Fire Station 8 site is known to have locally high aerosol concentrations (annual average higher by 1–2 $\mu g/m^3$). Fire Station 8 is located in a mixed industrial–commercial area with two large rail yards within ~200 m. A fire station and traffic intersection with significant diesel truck/automobile traffic are also located within ~50 m of the site. The Jefferson Street site is part of the Southeastern Aerosol Research and Characterization Study (SEARCH) and Aerosol Research Inhalation Epidemiology Study (ARIES). This site is located in a mixed commercial–residential area and has a characteristic urban signature [*Solomon et al.*, 2003]. A Greyhound bus maintenance facility with frequent diesel bus traffic during daytime hours and several busy roadways with traffic intersections are located within ~200 m of the site. *Hansen et al.* [2006] provides a detailed description of the site. Receptor modeling of PM2.5 total iron from this site has shown that it is mostly associated with vehicular, industrial, and crustal sources [*Liu et al.*, 2005].

[14] The PILS-LWCC was operated at Fire Station 8 during a 3 week fall period (16 November–8 December 2007) without the cyclone inlet (PM10), a 1 week spring period (16–22 April 2008), and a 3 week summer period (1–20 June 2008) with the cyclone installed (PM2.5). Ancillary measurements pertinent to the study included 5 min measurements of light-absorbing PM2.5 aerosol mass using an AE-16 single-channel aethalometer (Magee Scientific Company, Berkeley, California) and 1 min particle number concentration measurements using either a Condensation Particle Counter (CPC; TSI Incorporated, Shoreview, Minnesota) or an Optical Particle Counter (OPC; Met One, Grants Pass, Oregon) and meteorology parameters. Later in the summer (4 August–6 September 2008), the PILS-LWCC (PM2.5) was moved to the Jefferson Street site for the August Mini-Intensive Gas and Aerosol Study (AMIGAS) field campaign that included the deployment of several continuous aerosol and gas-phase measurements. Semicontinuous measurements of PM2.5 major inorganic anions (SO_4^{2-}, NO_2^-, NO_3^-, Cl^-) and cations (NH_4^+, Na^+, K^+, Ca^{2+}) were provided by a PILS coupled to an ion chromatograph (PILS-IC) [*Orsini et al.*, 2003]. Five minute averages of criteria gases (SO_2, O_3, and NO_y), meteorological parameters, PM2.5 mass concentrations (TEOM; Thermo Fisher Scientific Inc., Waltham, Massachusetts), and 1 h averages of light-absorbing aerosol (Aethalometer, Model RTA8, Magee Scientific Company, Berkeley, California) were provided by the existing techniques deployed for the SEARCH study.

2.2.3. Biomass Burning Study: Ichauway, Georgia

[15] A prescribed burn performed in early March 2008 in a longleaf pine and wiregrass forested region (~400 acres) provided the opportunity to characterize WS_Fe(II) emissions from biomass burning. These prescribed burning activities were in Ichauway, Georgia (31.276°N, −84.472°W), and organized by the Joseph W. Jones Ecological Research Center. The PILS-LWCC (PM2.5) and a suite of sampling instruments were deployed directly adjacent to the burn area to characterize aerosol and gaseous emissions. Water soluble potassium (PM2.5), a tracer for biomass burning, was measured in 8 min integrals by an electrochemical technique using an additional PILS. An Optical Particle Counter (Met One, Grants Pass, Oregon) provided 1 min size-resolved number concentration (0.3–2.5 μm).

3. Results and Discussion

3.1. Dearborn Measurements: Urban/Industrial Site in Winter

[16] The January 2008 Dearborn LADCO study afforded an opportunity to measure PM2.5 WS_Fe(II) in an industrial

Table 1. WS_Fe(II) Statistics for All Measurements at the Various Sampling Sites During Different Seasons[a]

Season	Sample Period	PM Size	Min	Max	% Below LOD[b]	Mean	Med	Std Dev	*N*
Fall Atlanta FS8	16 November 2007–6 December 2007	PM10	LOD	195	4.6	34.8	24.2	30.5	1401
Spring Atlanta FS8	16–22 April 2008	PM2.5	LOD	64.5	27.0	14.8	10.5	13.7	456
Summer Atlanta FS8	1–20 June 2008	PM2.5	LOD	356.1	36.7	13.4	6.9	28.3	2050
Summer Atlanta AMIGAS JST	10 August 2008–6 September 2008	PM2.5	LOD	41.8	49.7	5.1	4.6	3.6	1278
Dearborn, Michigan LADCO	19 January 2008–8 February 2008	PM2.5	LOD	434	30.2	17.7	9.8	26.3	1458

[a]All concentrations are presented in nanograms per meter cubed at ambient temperature and pressure.
[b]LOD are included as a value of 1/2 LOD.

setting during winter when atmospheric photochemical processes are expected to be at a minimum. Measurements of WS_Fe(II) were taken during a roughly 2 week sampling period when the mean temperature was −3.3°C, but ranged widely from −14.3°C to 17°C. Mean and median concentrations of PM2.5 WS_Fe(II) during the study were 17.7 and 9.8 ng m^{-3}, respectively (see Table 1). The data show significant temporal variability (Figure 1), with concentrations ranging from below the detection limit (LOD) to 434 ng m^{-3}. During episodes of snowfall, representing roughly 30% of the data, PM2.5 WS_Fe(II) concentrations were typically below the detection limit of 4.6 ng m^{-3}, likely due to the wet deposition of WS_Fe(II) (Figure 1). The data suggest a regional background concentration of approximately 10 ng m^{-3} with frequent PM2.5 WS_Fe(II) peaks (eight peaks in an 18 day period) ranging from 50 to 400 ng m^{-3} lasting for 6–12 h. No correlation was found between PM2.5 WS_Fe(II) and PM2.5 mass concentration during these peaks (R^2 = 0.004, N = 48 for eight transient events), indicating that the observed WS_Fe(II) was not linked to any other major PM2.5 chemical component. These higher PM2.5 WS_Fe(II) concentration events typically occurred during low wind speed periods (Figure 1) suggesting influences from local emissions. The wind roses of Figure 2 show that highest wind speeds were predominately from the southwest, but highest concentrations were mainly from the south. Industrial sources located within 10 km to the south of the site include a coal-fired power plant, a cement kiln, a large petroleum refinery, a wastewater treatment plant, and two steel mills. Correlation between PM2.5 EC or OC and PM2.5 WS_Fe(II) throughout the study were not significant (R^2 = 0.03 and 0.12, respectively, N = 323 (for both EC and OC analysis), based on 12 min WS_Fe(II) merged to the 48 min OC and EC measurements) indicating that industrial emissions likely influenced PM2.5 WS_Fe(II) rather than mobile emissions.

3.2. Atlanta: Measurements During Various Seasons

3.2.1. Overall Seasonal Variability and Transient Events

[17] Measurements of WS_Fe(II) were completed in Atlanta, Georgia, at Fire Station 8 during three different seasons to investigate seasonal and temporal variability. In addition to these measurements, the AMIGAS study during August/September 2008 in Atlanta provided an opportunity to measure WS_Fe(II) simultaneously with several other atmospheric tracer species for a more comprehensive investigation of sources. Statistical summaries of WS_Fe(II) measurements at the Atlanta sites are given in Table 1.

[18] The median WS_Fe(II) concentrations recorded at the Atlanta Fire Station 8 site during fall, spring, and summer were typically from LOD to 24.2 ng m^{-3}, for both PM10 and PM2.5, with highest concentrations in the fall associated with

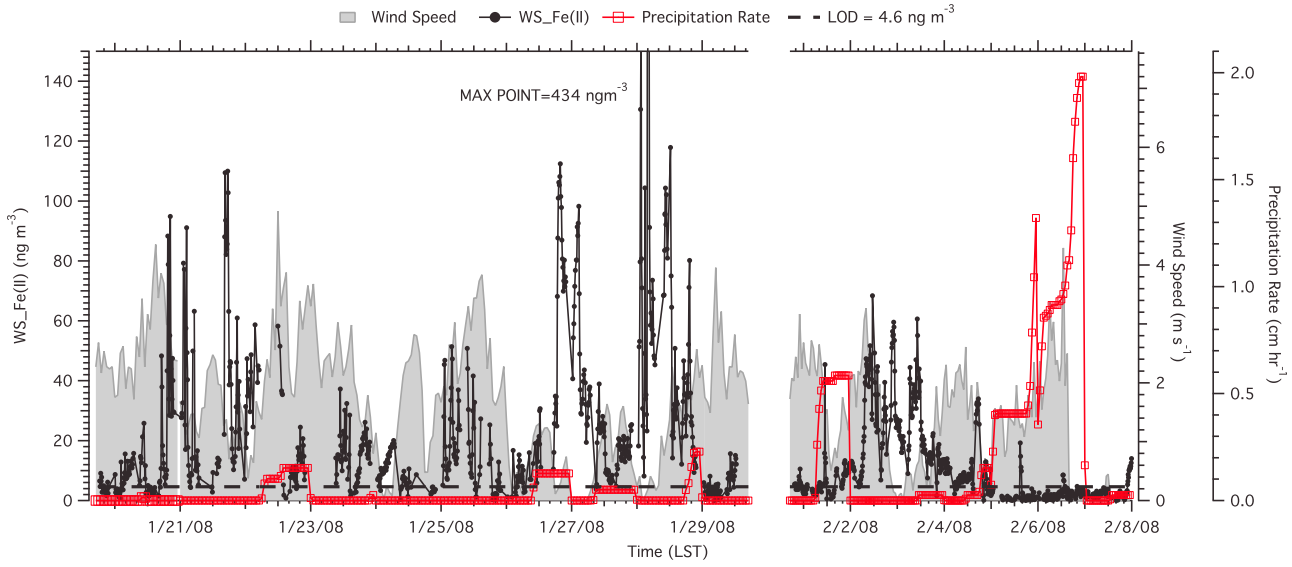

Figure 1. Time series of PM2.5 WS_Fe(II) (black dotted line) and wind speed (shading) in Dearborn, Michigan, during part of the 1 month study. The WS_Fe(II) LOD of 4.6 ng m^{-3} and precipitation rate is indicated by the dashed black line and red open square line, respectively.

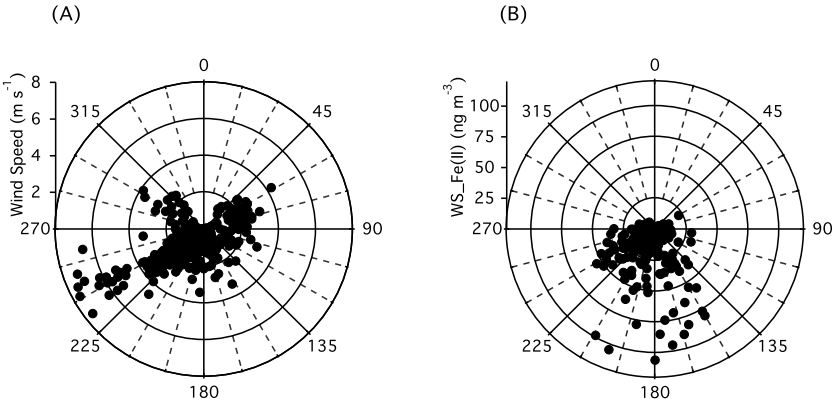

Figure 2. Wind rose plots for the Dearborn, Michigan study showing hourly mean meteorological parameters and PM2.5 WS_Fe(II) concentration. (a) Wind speed (m s^{-1}) versus wind direction, (b) PM2.5 WS_Fe (II) concentration (ng m^{-3}) versus wind direction (a data point, 434 ng m^{-3}, is off scale).

PM10. The measured levels are of similar magnitude to those reported for PM10 soluble (total = II + III) iron in Los Angeles, California; East St. Louis, Illinois; and Waukesha, Wisconsin (from 0.4 to 11 ng m^{-3}) [*Majestic et al.*, 2007] and downwind of China (TSP 32 ng m^{-3}) [*Chuang et al.*, 2005]. However, these concentrations are roughly 1 to 2 orders of magnitude higher than fine and coarse levels of WS_Fe(II) recorded in remote marine regions [*Johansen et al.*, 2000; *Siefert et al.*, 1999]. Fire Station 8 median concentrations tended to be higher in spring compared to summer, and lowest concentrations (median: 4.6 ± 3.6 ng m^{-3}) were observed in August and September during the AMIGAS study at the Jefferson Street site. The observed seasonal variability could be associated with differences in meteorology (e.g., prevalent wind direction, boundary layer height) or chemical processes, such as enhanced summertime photochemistry and oxidant concentrations shifting iron away from the Fe(II) oxidation state [*Sedlak et al.*, 1997]. However, there is evidence for redox chemistry playing a role in the WS_Fe(II) seasonal trend since an extensive data set of total water soluble iron collected from 24 h integrated Federal Reserve Method FRM filters consistently shows higher total water soluble Fe in summer (mean: 40–50 ng m^{-3} for June, July, August) compared to fall/winter months (mean: 15–20 ng m^{-3} for November, December, January, February) for several years. In this method, iron was quantified by Inductively Coupled Plasma–Optical Emission Spectroscopy (ICP–OES) or Inductively Coupled Plasma–Atomic Absorption Spectroscopy (ICP–AAS) on aliquots obtained through aqueous extraction of FRM filters. Although the difference in our WS_Fe(II) and the total water soluble iron seasonal trend may be caused by differences in analytical techniques (ICP-OES/ICP-AAS versus UV/VIS) and/or sample extraction (filter vs. PILS), it may also be a direct result of WS_Fe(II) shifting to a more oxidized state at times when photochemistry and oxidant concentrations are expected to be enhanced (e.g., summer).

[19] The Atlanta Fire Station 8 data sets exhibited high temporal variability in all seasons with concentrations ranging from the LOD to approximately 200 ng m^{-3} in the fall, and LOD to approximately 350 ng m^{-3} in the summer. Figure 3 shows a time series of a multiday period during November (PM10) and June (PM2.5), both at Fire Station 8. In November, WS_Fe(II) concentrations varied during all hours of the day (Figure 3a), a feature that was also observed in the spring data set (data not shown). In contrast, temporal variability during June measurements was largely driven by unique transient PM2.5 WS_Fe(II) events that generally occurred in the early evening and lasted for approximately 1–2 h. Peak concentrations reached ~200–350 ng m^{-3}, which were superimposed on a low WS_Fe(II) background of ~10 ng m^{-3} that was present for most of the day. These events consistently occurred over roughly a 16 day period and then ended. A dramatic decrease in wind speed roughly 1–2 h prior to these events was also observed (Figure 3b). Although wind directions were variable at these peak WS_Fe(II) peak times (consistent with low wind speeds), most peaks were associated with winds from the southern quadrants (southeast to southwest). For a short period (2–3 days) during these events, measurements were made of particle number concentrations with a CPC (D_p range: 0.01 to > 1 μm) and OPC (D_p range: 0.3 to > 5 μm). PM2.5 WS_Fe(II) peaks tracked well with the CPC data but not with the OPC data, suggesting increases only in the ultrafine particle number concentration (sizes below ~0.1 μm diameter). In addition, no correlation was observed between PM2.5 WS_Fe(II) and the light-absorbing aerosol (e.g., soot; $R^2 = 0.0001$, $N = 101$, for a total of seven events). The combination of correlation with ultrafine particle number concentrations and lack of correlation with black carbon suggests that these WS_Fe(II)-rich particles were associated with fresh combustion-related activity but were likely not related to internal combustion engines (mobile sources). Due to the clockwork nature of these transient events around 2000 to 2200 every night, these events appear to be related to a regular activity occurring near the sampling site.

3.2.2. Transient Events: WS_Fe(II), SO_2, SO_4^{2-} and Particle Acidity

[20] Additional transient PM2.5 WS_Fe(II) events were observed in Atlanta during the 1 month (August–September 2008) AMIGAS study at Jefferson Street, but with much smaller peak concentrations (typically 10–40 ng m^{-3}). Because this intensive study involved continuous real-time measurement of trace gas and aerosol composition, a more detailed

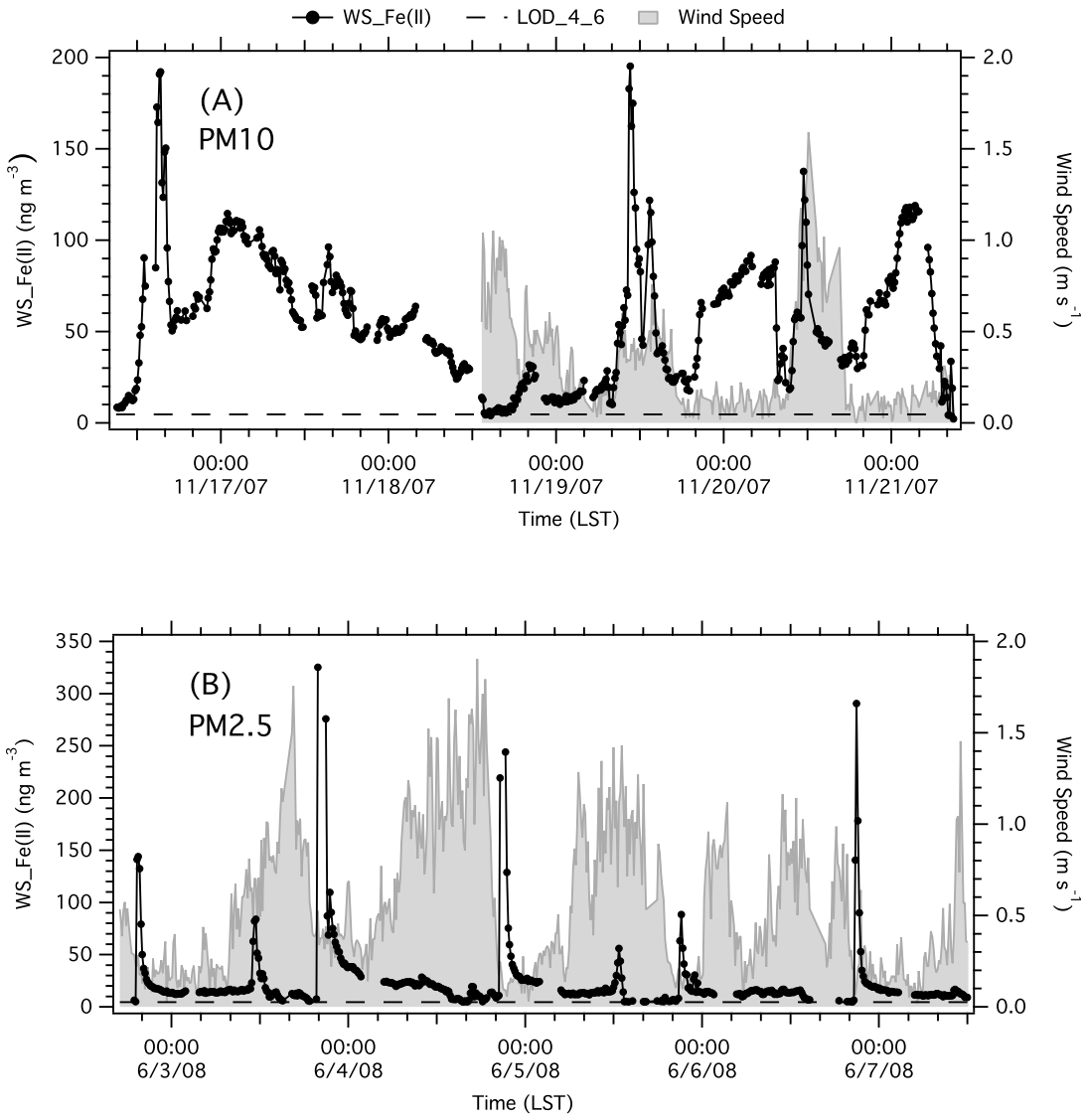

Figure 3. Examples of WS_Fe(II) time series measured in Atlanta for 5 day periods during (a) fall and (b) summer. The dotted black line represents WS_Fe(II) concentration, and the dashed black line represents WS_Fe(II) LOD (4.6 ng m^{-3}). Wind speeds are also plotted (shading) when data are available.

analysis of the source of the observed WS_Fe(II) peaks was feasible. These WS_Fe(II) events occurred during a 3 day period when wind speeds (~2.5 m s^{-1}) were low, and the highest PM2.5 mass concentrations (~34 μg m^{-3}) were observed, suggesting stagnant atmospheric conditions. In addition, the average PM2.5 sulfate (SO_4^{2-}) concentration increased to ~7–10 μg m^{-3} from typical concentrations of ~2–4 μg m^{-3}. In general, these transient WS_Fe(II) events tracked well with mid to late afternoon peaks in PM2.5 SO_4^{2-} concentration that were associated with SO_2 peaks. Similar late afternoon SO_4^{2-} peaks have been observed in Atlanta during the summer and are thought to result from the entrainment of relatively nearby coal-fired power plant SO_2 emissions into the expanding daytime planetary boundary layer, combined with afternoon photochemical production of SO_4^{2-} [*Weber et al.*, 2003]. These events also tracked well with PM2.5 mass data (data not shown), which is consistent with large increases of PM2.5 SO_4^{2-}, a major component of PM2.5 in Atlanta. Figure 4 shows the average diurnal trends for SO_2, SO_4^{2-}, and WS_Fe(II) (based on hourly averaged data), and indicates that for all three compounds, increases in concentrations were most often observed during late afternoon.

[21] Figure 5 shows real-time measurements of SO_2, SO_4^{2-} and WS_Fe(II) compounds for the 3 day period during the AMIGAS study. Although the SO_4^{2-} peaks followed SO_2 maxima data, the relative proportions in peak heights varied. Differences in proportions of SO_2 and SO_4^{2-} for the various plumes can be attributed, at least in part, to differences in photochemical aging, where more aged plumes are expected to have higher SO_4^{2-} relative to SO_2 due to photochemical conversion of SO_2 to SO_4^{2-}. Photochemical age, for example,

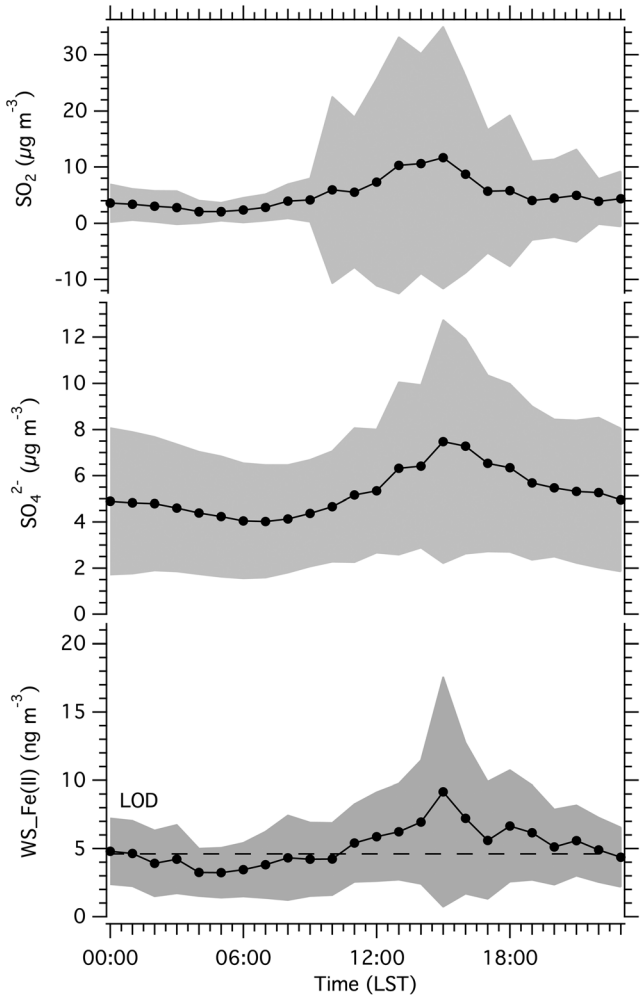

Figure 4. Mean (dotted black line) and plus/minus one standard deviation (shading) of hourly averaged data for PM2.5 WS_Fe(II), SO_4^{2-}, and SO_2 during August–September 2008 AMIGAS study in Atlanta. The dashed black line represents the WS_Fe(II) LOD (4.6 ng m^{-3}).

may account for the differences in proportions between SO_2 and SO_4^{2-} for peaks labeled A (more fresh) and B (more aged) in Figure 5. During this time period, peak concentrations of WS_Fe(II) tend to follow SO_4^{2-} but not SO_2. Event B exhibited the highest SO_4^{2-} and WS_Fe(II) concentrations recorded for the AMIGAS study, but the associated SO_2 maximum was clearly not the highest observed. These comparisons suggest that PM2.5 WS_Fe(II) was associated with the SO_2 plumes, but for the most part, WS_Fe(II) was not emitted directly along with SO_2. Several studies have shown that coal-fired power plant fly ash emissions contain iron [*Reddy et al.*, 2005; *Smith*, 1980], and this may be the source of the WS_Fe(II) observed here; however, other factors appear to influence the enhancement and/or stability of WS_Fe(II). A few studies suggest that aerosol acidity may play a role in enhanced WS_Fe(II) concentrations through an influence on iron solubility and stability [*Duce and Tindale*, 1991; *Meskhidze et al.*, 2003; *Zhuang et al.*, 1992]; however, one study observed no relationship between increased Fe solubility and atmospheric acidic species [*Baker et al.*, 2006]. At low pH values, the solubility of various forms of insoluble iron, such as iron oxides, is enhanced, and transformations between iron oxidation states are substantially slower; thus, WS_Fe(II) may persist in the particle for longer periods of time. During the AMIGAS study, it is possible that either WS_Fe(II) or insoluble iron was internally mixed with highly acidic SO_4^{2-} particles formed by SO_2 oxidation, resulting in either increased stability of WS_Fe(II) or the mobilization of insoluble iron to WS_Fe(II).

[22] For a more comprehensive analysis, SO_2 and WS_Fe(II) data for the entire AMIGAS study (August–September 2008) were merged onto the SO_4^{2-} measurement 20 min time scale. If SO_2 concentration increased four times the background concentration of 1 ppbv during the entire study, the peak was deemed a SO_2 transient event. For each SO_2 peak, the average concentration increase relative to background levels was determined for SO_2, SO_4^{2-}, and WS_Fe(II) (denoted as ΔSO_2, ΔSO_4^{2-}, and ΔWS_Fe(II)). For example,

$$\Delta \text{WS\_Fe(II)} = \frac{\sum \left(\text{WS\_Fe(II)}_i - \text{WS\_Fe(II)}_b\right)}{n},$$

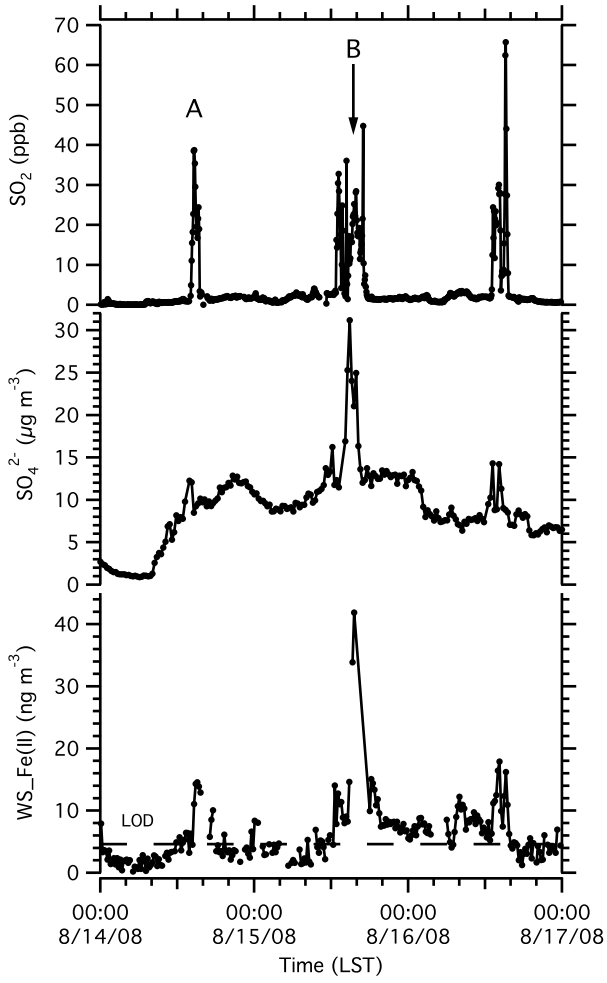

Figure 5. Sample time series during a 3 day period of the AMIGAS study showing transient SO_2 events and corresponding PM2.5 SO_4^{2-} and WS_Fe(II).

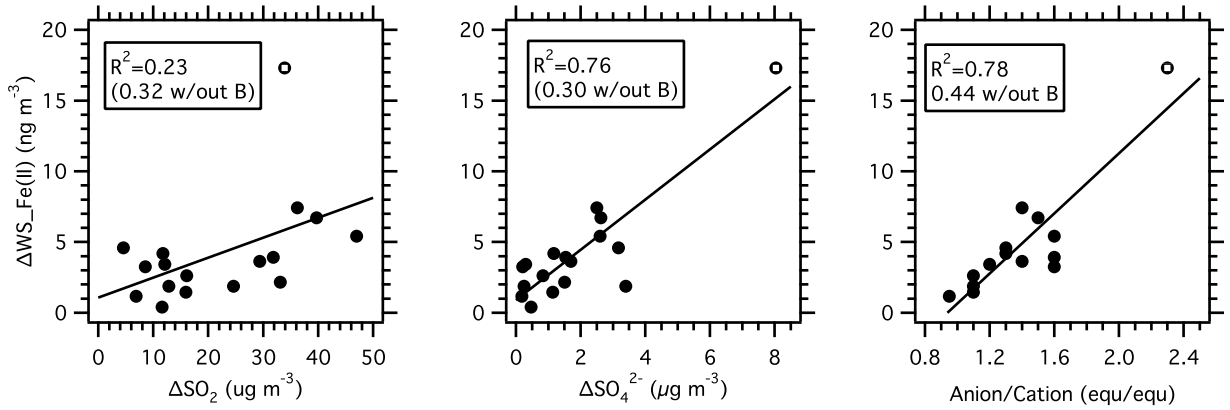

Figure 6. ΔWS_Fe(II) correlation to ΔSO_2, ΔSO_4^{2-}, and the anion/cation equivalence ratio for each of the 17 SO_2 peaks observed during AMIGAS. ΔWS_Fe(II) is the average WS_Fe(II) concentration increase relative to background concentrations (average of WS_Fe(II) recorded at the time just before and after the SO_2 peak). For each plot the coefficient of determination (R^2) is given for all data and when the largest peak during Event B (open circle, also see Figure 5) is excluded.

where $WS\_Fe(II)_i$ is the concentration recorded in the peak, $WS\_Fe(II)_b$ is the average of the WS_Fe(II) concentration measured at the time just prior to and after the SO_2 peak, and n is the number of measurements made within the WS_Fe (II) peak. In addition to this analysis, the degree of aerosol acidity was assessed through an ion balance between the suite of measured PM2.5 anions and cations, since aerosol pH was not directly measured. Studies in Atlanta have shown that the major ions associated with fine particles are SO_4^{2-} and NH_4^+, with much smaller amounts of NO_3^- [*Solomon et al.*, 2003]. Other ions (i.e., crustal elements) are only minor components of Atlanta PM2.5 and do not significantly contribute to the ion balance [*Solomon et al.*, 2003]. Ratios of $(SO_4^{2-} + NO_3^-)/NH_4^+$ in equivalence units that are greater than one result from an excess of SO_4^{2-} and NO_3^- relative to NH_4^+, which is likely balanced by the unmeasured H^+ cation and correspond to an acidic aerosol. Aerosol particles near neutral will have anion/cation equivalent ratios near one.

[23] A total of 17 SO_2 peaks were observed during the study, and Figure 6 shows the ΔWS_Fe(II) correlations with ΔSO_2, ΔSO_4^{2-}, and the anion/cation ratio for each peak. Unfortunately, during AMIGAS, there were few large sulfate peaks; thus, the correlations tend to be dominated by the one major peak (event B) observed in the afternoon of 15 August 2008, when the relative change in SO_4^{2-} concentration was ~8 μg m^{-3} compared to other peaks where the change was in the range of 1–2 μg m^{-3}. The results show a general increasing trend between ΔWS_Fe(II) and apparent aerosol acidity. The correlation with SO_4^{2-} is also expected, since plumes with highest sulfate are likely to be the most acidic, due to titration of all available neutralizing ammonia.

[24] These data also suggest that the PM2.5 WS_Fe(II) and sulfate were internally mixed (present in same particles), which in turn would imply that most WS_Fe(II) was associated with accumulation mode particles (the size that most secondary sulfate particles occur). Given that the PILS-LWCC only measures WS_Fe(II) and no other online WS_Fe(III) and total Fe were available during the AMIGAS study, the exact sources of the iron in these plumes cannot be identified. Thus, we cannot determine whether WS_Fe(II) or some form of iron that was later acid-processed to WS_Fe(II) was coemitted with SO_2. However, WS_Fe(II) does not appear to have been emitted directly with the SO_2. It is also possible that catalytic conversion of SO_2 to SO_4^{2-} in aqueous drops containing H_2O_2 by Fe(II) [*Breytenbach et al.*, 1994] may have played a role.

[25] The influence of SO_2 plumes in the transient PM2.5 WS_Fe(II) events observed at Fire Station 8 cannot be assessed since comparable time-resolved SO_2 or aerosol SO_4^{2-} measurements are not available. However, most of the June Fire Station 8 events shown in Figure 3b were different from those observed during the AMIGAS study, both in magnitude and timing. In general, the Fire Station 8 peak concentrations were significantly greater and were typically observed much later in the day, often near midnight, thus suggesting different sources or methods of processing of WS_Fe(II).

3.2.3. Diurnal Variability and Photochemical Processes

[26] Some studies have observed diurnal variability in WS_Fe(II), possibly driven by photochemical processes. For example, *Willey et al.* [2000] attributed daytime increases in rainwater Fe(II) measurements to photoreduction processes. This well-studied mechanism for the formation of WS_Fe(II) in atmospheric liquid water involves conversion of Fe(III) complexed to specific organic acids (i.e., carboxylic acid moieties) through a ligand-to-metal charge transfer yielding reduced iron and an oxidized organic complex [*Pehkonen et al.*, 1993]. Other studies focusing on cloud water samples, however, have not observed a diurnal trend of WS_Fe(II) that is indicative of photochemical activity [*Parazols et al.*, 2006].

[27] To investigate if a persistent diurnal pattern in WS_Fe(II) was present in our measurements, the data for each season was binned into hourly mean WS_Fe(II) concentrations. Figure 7 shows the diurnal variability for the Atlanta measurements during three different seasons. Specific transient WS_Fe(II) events were removed from the data set prior to binning and averaging the data that were apparently associated with a source other than photoreductive processes, such as the late evening transient events during the summer at Fire Station 8 (Figure 7c), and all WS_Fe(II) associated with the SO_2 events during the AMIGAS study (Figure 7d). All other

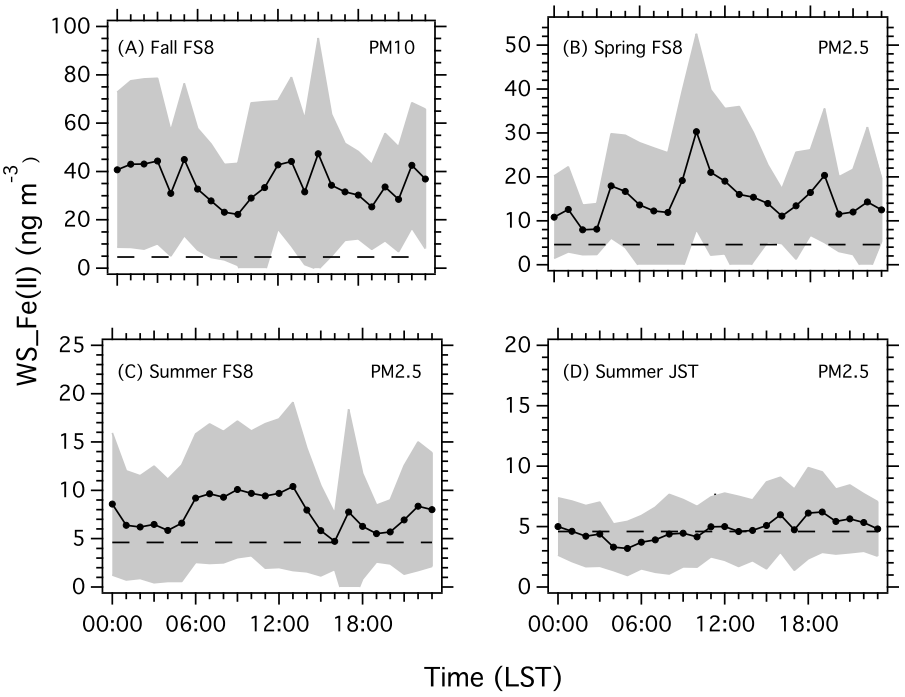

Figure 7. Diurnal trends during different seasons in Atlanta, Georgia. For each plot, the dotted black line represents mean hourly WS_Fe(II) concentration and the shaded area is plus/minus one standard deviation. The dashed black line represents the WS_Fe(II) LOD. FS8 stands for Fire Station 8 site, and JST stands for Jefferson Street site. Transient events were removed from Summer FS8 and Summer JST data prior to binning and averaging.

data are included in the averages plotted in Figure 7. Based on this analysis, no net increase in WS_Fe(II) concentration was observed during the daytime; therefore, we conclude that iron photoreductive processes do not appear to have a significant net effect on the ambient WS_Fe(II) concentration during the periods studied at these sites. However, it is possible that WS_Fe(II) was formed by photoreductive processes during the study and then counterbalanced by the WS_Fe(II) lost from oxidative processes, resulting in no net increase in ambient concentrations during daytime hours.

3.2.4. Mobile Sources: WS_Fe(II) and Light-Absorbing Aerosol

[28] As discussed above, no correlation was observed between PM2.5 light-absorbing aerosol (or elemental carbon) and WS_Fe(II) during the wintertime at Dearborn, Michigan. A similar result was observed in Atlanta throughout all the measurements at the Fire Station 8 and Jefferson Street sites (R^2 = 0.34, N = 744 fall (FS8); R^2 = 0.04, N = 342 spring (FS8); R^2 = 0.004, N = 1637 summer (FS8); R^2 = 0.01, N = 535 summer (AMIGAS), based on 5 min measurements of light-absorbing aerosol merged to WS_Fe(II) 12 min data at FS8 and 12 min WS_Fe(II) data merged to 1 h light-absorbing aerosol data for AMIGAS). However, there are studies showing a link between iron, mobile sources [*Hammond et al.*, 2008; *Majestic et al.*, 2009], and EC [*Chuang et al.*, 2005]. *Chuang et al.* [2005] found a strong relationship between 24 h integrated WS_Fe, believed to be primarily WS_Fe(II), and EC (R^2 = 0.7) as well as no association between enhanced iron solubility and mineral dust events based on measurements from Cheju, Korea. They conclude that the WS_Fe was better associated with the long-range transport of Asian anthropogenic emissions related to combustion processes rather than processing of mineral dust. We do not view these results as contradictory to our results. Although EC is mainly linked to mobile emissions (in the absence of biomass burning) in North America [*Schauer*, 2003, and references therein], this is not the case in Asia, where it can be associated with coal or other forms of fossil fuel emissions [*Streets et al.*, 2001]. For our sampling sites, mobile sources were not directly linked to enhanced WS_Fe(II) concentrations. In *Chuang et al.* [2005], EC is not used as a specific tracer of mobile sources, but rather as a more general tracer of Asian anthropogenic emissions. Another possibility for the poor correlation between EC and WS_Fe(II) during our sampling periods may be that soluble iron from mobile sources is predominately emitted as WS_Fe(III). Our findings combined with those by *Chuang et al.* [2005] highlight that more studies in different regions are required before we can accurately assess the relationship between combustion sources and water soluble iron.

3.3. Impact of Biomass Burn Aerosols on Urban WS_Fe(II) Spatial Distribution

[29] Studies have reported total iron concentrations in biomass burning emissions, which is typically a small portion (i.e., less than 1%) of total burn emissions [*Chen et al.*, 2007; *Lee et al.*, 2005; *Yamasoe et al.*, 2000]. One study hypothesized that biomass-burning emissions may be a direct source of water soluble iron in aerosols. This same study further concluded that pyrogenic sources have only a minor impact on the atmospheric flux of soluble iron to the atmosphere

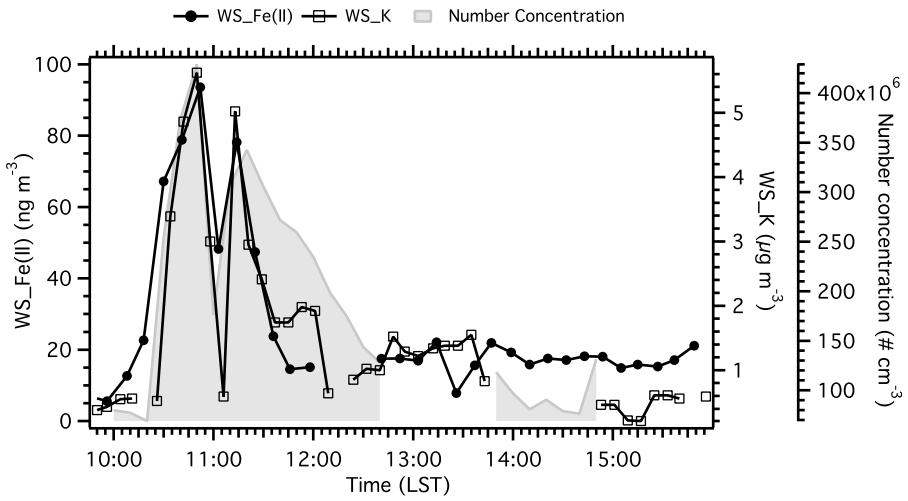

Figure 8. PM2.5 WS_Fe(II) (dotted black line), Optical Particle Counter number concentration (particles larger than 0.3 μm diameter: shading), and fine particle WS_K (black open square line) during a prescribed burn in Ichauway, Georgia, when the site was impacted by two plumes.

(8.3×10^9 g yr^{-1}), representing roughly 10% of soluble iron from arid regions [*Guieu et al.*, 2005].

[30] In this study, measurements of PM2.5 WS_Fe(II) were made in a prescribed burn to characterize fire emissions and determine whether these emissions could have an impact on Atlanta WS_Fe(II) concentrations. Figure 8 shows a time series of particle number concentration (sizes between 0.3 to 2.5 μm diameter), PM2.5 water soluble potassium (WS_K), and PM2.5 WS_Fe(II) during one period of the prescribed burning. A clear relationship between WS_Fe(II) and WS_K, a known marker for biomass burning [*Andreae*, 1983], shows that PM2.5 WS_Fe(II) is associated with biomass-burning emissions. In these experiments, WS_Fe(II) and WS_K were highly correlated (R^2 = 0.88, N = 17), and based on linear regression, the emission ratio of WS_Fe(II) relative to WS_K was estimated at 15 ± 2 mg/g (intercept of 2.7 ± 3.1 ng m^{-3}).

[31] Even within the region of burning, the highest PM2.5 WS_Fe(II) concentration observed was only 94 ng m^{-3}. In comparison to the urban measurements, this is less than peak WS_Fe(II) levels recorded in Atlanta (~200–300 ng m^{-3}) or Dearborn (~400 ng m^{-3}), suggesting that biomass burning likely did not significantly contribute to the large transient events observed (this is also consistent with lack of correlation with light-absorbing aerosol or EC).

[32] Wood burning also likely did not significantly contribute to the background (regional) concentrations of WS_Fe(II) observed in Atlanta. For example, using the above emission ratio, and an analysis of 2007 FRM filters in urban Atlanta (South Dekalb, Georgia, Environmental Protection Division (EPD) site), during winter when biomass burning is most prevalent, a recorded mean WS_K concentration of 0.043 μg m^{-3} corresponds to a PM2.5 WS_Fe(II) concentration of only 0.7 ng m^{-3}, which is below our instrument detection limit. Moreover, in the spring of 2007, extensive fires in southern Georgia at times severely impacted Atlanta air quality over extended time periods. Based on 24 h integrated filter measurements, maximum WS_K concentrations of 0.1 μg m^{-3} correspond to a WS_Fe(II) concentration of only 1.6 ng m^{-3}. Although this analysis is highly uncertain, when it is considered along with the relatively low PM2.5 WS_Fe(II) concentrations recorded next to the fires, it suggests that biomass burning was likely not an important contributor to the WS_Fe(II) measured in the urban regions of this study. Significant influence of biomass burning on ambient WS_Fe(II) concentrations are likely limited to regions that experience extensive forest fire impact in otherwise pristine environments.

4. Summary

[33] To date, filter-based measurements with long (e.g., 24 h) integration times have been used to quantify WS_Fe(II) and characterize sources in various environments. This study presents the first continuous and near-real time WS_Fe(II) measurements from a number of sites. The following findings are reported:

[34] 1. Typical background PM10 and PM2.5 WS_Fe(II) concentrations recorded in Atlanta, Georgia, and Dearborn, Michigan, were on the order of tens of nanograms per cubic meter, which is comparable to WS_Fe(II) measured in other urban areas based on integrated filter sampling techniques.

[35] 2. Sampling at the various sites in Atlanta, Georgia, during different seasons suggests a general trend: highest mean WS_Fe(II) concentrations were observed in fall/winter (mean: 34.8 ± 30.6 ng m^{-3}) and lowest concentrations recorded in summer (mean: 5.1 ± 3.6 ng m^{-3}). Integrated filter measurements in Atlanta, however, have shown an opposite seasonal trend for total water soluble iron, with highest concentrations in the summer. These combined results may be linked to a higher conversion rate of WS_Fe(II) to oxidized forms of iron during periods of higher oxidant concentrations (e.g., summer).

[36] 3. High WS_Fe(II) concentrations were typically associated with frequent transient WS_Fe(II) events (~1–12 h) at the urban sampling sites in this study. In Dearborn, event concentrations ranged from 100 to 400 ng m^{-3} and were likely associated with local industrial activity. At Fire Station 8 in Atlanta, unique summertime WS_Fe(II) transient event concentrations ranged from 200 to 350 ng m^{-3} and appeared to be linked to fresh combustion-generated particles from some unidentified activity near the site. Several transient

WS_Fe(II) events in Atlanta were also found to be associated with SO_4^{2-} and SO_2 peaks, with a general increasing trend of ambient WS_Fe(II) concentrations with apparent particle acidity. However, the actual source of iron in the transient events at both the Detroit and Atlanta sites could not be identified with our data set.

[37] 4. Daily 1 h averages of WS_Fe(II) concentrations at all urban locations and seasons showed no evidence for a significant or consistent diurnal trend, suggesting that photoreductive processes did not result in a significant net increase in ambient concentrations of WS_Fe(II) during our study periods.

[38] 5. A poor correlation between WS_Fe(II) and light-absorbing aerosol (or elemental carbon) was observed at all urban sites during all seasons, indicating that mobile source emissions are not directly linked to enhanced WS_Fe(II) concentrations.

[39] 6. WS_Fe(II) was associated with biomass-burning emissions based on a strong relationship observed between WS_Fe(II) and WS_K (R^2 = 0.88). An emission ratio of WS_Fe(II)/WS_K = 15 mg/g (N = 17) was estimated based on measurements within a prescribed burn of longleaf pine and wiregrass in southern Georgia. Although significant WS_Fe(II) increases in concentration were observed within the prescribed burn (WS_Fe(II) range: 5–94 ng m^{-3}), the highest recorded WS_Fe(II) concentration near the burn region was less than typical transient events in Atlanta. Biomass burning likely impacts WS_Fe(II) in regions with high biomass burning activity; however, it is not believed to have had a significant influence on WS_Fe(II) in the urban regions we studied.

[40] **Acknowledgments.** The authors would like to thank the U.S. Environmental Protection Agency (EPA) for its financial support of this project under STAR Research Grant RD-83283501. The views expressed in this document are solely those of the authors, and EPA does not endorse any of the products or commercial services mentioned in the publication. We gratefully acknowledge David Snyder who provided a source inventory for Dearborn, Michigan, Xiaolu Zhang who provided FRM filter measurements of WS_K, and Armistead Russell who provided meteorological and elemental carbon data from Fire Station 8. PILS-IC data used during AMIGAS were supported by the Electric Power Research Institute (EPRI) through contract EP-P28304/C13438, and the Georgia prescribed burning study was funded by the Georgia Department of Natural Resources (DNR) through contract 773–80164. Measurements at the various sites were made possible through logistical support offered by the Michigan Department of Environmental Quality during the 2008 LADCO winter field campaign, by Armistead Russell for the use of the ASACA Fire Station 8 site, by EPRI's Stephanie Shaw and SEARCH personnel (John Jansen) for use of the Jefferson Street site during the AMIGAS field campaign, and by the staff at Joseph W. Jones Ecological Research Center and Georgia EPD for the fire study.

References

Alexander, B., R. J. Park, D. J. Jacob, and S. Gong (2009), Transition metal-catalyzed oxidation of atmospheric sulfur: Global implications for the sulfur budget, *J. Geophys. Res.*, *114*, D02309, doi:10.1029/2008JD010486.

Andreae, M. O. (1983), Soot carbon and excess fine potassium: Long-range transport of combustion-derived aerosols, *Science*, *220*, 1148–1151, doi:10.1126/science.220.4602.1148.

Baker, A. R., et al. (2006), Trends in the solubility of iron, aluminum, manganese and phosphorus in aerosol collected over the Atlantic Ocean, *Mar. Chem.*, *98*, 43–58, doi:10.1016/j.marchem.2005.06.004.

Brandt, C., and R. van Eldik (1995), Transition metal-catalyzed oxidation of sulfur (IV) oxides. Atmospheric-relevant processes and mechanisms, *Chem. Rev.*, *95*, 119–190, doi:10.1021/cr00033a006.

Breytenbach, L., et al. (1994), The influence of organic acids and metal ions on the kinetics of the oxidation of sulfur(IV) by hydrogen peroxide, *Atmos. Environ.*, *28*(15), 2451–2459, doi:10.1016/1352-2310(94)90396-4.

Chen, L.-W. A., et al. (2007), Emissions from laboratory combustion of wildland fuels: Emission factors and source profiles, *Environ. Sci. Technol.*, *41*(12), 4317–4325, doi:10.1021/es062364i.

Chen, Y., and R. L. Siefert (2004), Seasonal and spatial distributions and dry deposition fluxes of atmospheric total and labile iron over the tropical and subtropical North Atlantic Ocean, *J. Geophys. Res.*, *109*, D09305, doi:10.1029/2003JD003958.

Chuang, P. Y., et al. (2005), The origin of water soluble particulate iron in the Asian atmospheric outflow, *Geophys. Res. Lett.*, *32*, L07813, doi:10.1029/2004GL021946.

Claquin, T., et al. (1999), Modeling the mineralogy of atmospheric dust sources, *J. Geophys. Res.*, *104*(D18), 22,243–22,256, doi:10.1029/1999JD900416.

Duce, R. A., and N. W. Tindale (1991), Atmospheric transport of iron and its deposition in the ocean, *Limnol. Oceanogr.*, *36*(8), 1715–1726.

Erel, Y., S. O. Pehkonen, and M. R. Hoffmann (1993), Redox chemistry of iron in fog and stratus clouds, *J. Geophys. Res.*, *98*(D10), 18,423–18,434, doi:10.1029/93JD01575.

Faust, B. C., and J. Hoigne (1988), Photolysis of Fe(III)-hydroxy complexes as a source of hydroxyl radicals in atmospheric waters, *Atmos. Environ.*, *24*(1), 79–89.

Faust, B. C., and R. G. Zepp (1993), Photochemistry of aqueous iron(III)–polycarboxylate complexes: Roles in the chemistry of atmospheric and surface waters, *Environ. Sci. Technol.*, *27*(12), 2517–2522, doi:10.1021/es00048a032.

Gao, Y., et al. (2003), Aeolian iron input to the ocean through precipitation scavenging: A modeling perspective and its implication for natural iron fertilization in the ocean, *J. Geophys. Res.*, *108*(D7), 4221, doi:10.1029/2002JD002420.

Guieu, C., et al. (2005), Biomass burning as a source of dissolved iron to the open ocean? *Geophys. Res. Lett.*, *32*, L19608, doi:10.1029/2005GL022962.

Hammond, D. M., et al. (2008), Sources of ambient fine particulate matter at two community sites in Detroit, Michigan, *Atmos. Environ.*, *42*(4), 720–732, doi:10.1016/j.atmosenv.2007.09.065.

Hansen, D. A., et al. (2006), Air quality measurements for the aerosol research and inhalation epidemiology study, *J. Air Waste Manag. Assoc.*, *56*(10), 1445–1458.

Jickells, T. D., et al. (2005), Global iron connections between desert dust, ocean biogeochemistry, and climate, *Science*, *308*(5718), 67–71, doi:10.1126/science.1105959.

Johansen, A. M., et al. (2000), Chemical composition of aerosols collected over the tropical North Atlantic Ocean, *J. Geophys. Res.*, *105*(D12), 15,277–15,312, doi:10.1029/2000JD900024.

Journet, E., et al. (2008), Mineralogy as a critical factor of dust iron solubility, *Geophys. Res. Lett.*, *35*, L07805, doi:10.1029/2007GL031589.

Kelly, F. J. (2003), Oxidative stress: Its role in air pollution and adverse health effects, *Occup. Environ. Med.*, *60*(8), 612–616, doi:10.1136/oem.60.8.612.

Kidwell, C. B., and J. M. Ondov (2004), Elemental analysis of sub-hourly ambient aerosol collections, *Aerosol Sci. Technol.*, *38*(3), 205–218, doi:10.1080/02786820490261726.

Lam, P. J., and J. K. Bishop (2008), The continental margin is a key source of iron to the HNLC North Pacific Ocean, *Geophys. Res. Lett.*, *35*, L07608, doi:10.1029/2008GL033294.

Lee, S., et al. (2005), Gaseous and particulate emissions from prescribed burning in Georgia, *Environ. Sci. Technol.*, *39*(23), 9049–9056, doi:10.1021/es0515831.

Liu, W., et al. (2005), Atmospheric aerosol over two urban–rural pairs in the southeastern United States: Chemical composition and possible sources, *Atmos. Environ.*, *39*(25), 4453–4470, doi:10.1016/j.atmosenv.2005.03.048.

Majestic, B. J., et al. (2006), Development of a wet-chemical method for the speciation of iron in atmospheric aerosols, *Environ. Sci. Technol.*, *40*(7), 2346–2351, doi:10.1021/es052023p.

Majestic, B. J., et al. (2007), Application of synchrotron radiation for measurement of iron red-ox speciation in atmospherically processed aerosols, *Atmos. Chem. Phys.*, *7*(10), 2475–2487.

Majestic, B. J., A. D. Anbar, and P. Herckes (2009), Elemental and iron isotopic composition of aerosols collected in a parking structure, *Sci. Total Environ.*, *407*(18), 5104–5109, doi:10.1016/j.scitotenv.2009.05.053.

Meskhidze, N., et al. (2003), Iron mobilization in mineral dust: Can anthropogenic SO_2 emissions affect ocean productivity? *Geophys. Res. Lett.*, *30*(21), 2085, doi:10.1029/2003GL018035.

Orsini, D. A., et al. (2003), Refinements to the particle-into-liquid sampler (PILS) for ground and airborne measurements of water soluble aerosol composition, *Atmos. Environ.*, *37*(9–10), 1243–1259, doi:10.1016/S1352-2310(02)01015-4.

Parazols, M., et al. (2006), Speciation and role of iron in cloud droplets at the puy de Dôme station, *J. Atmos. Chem.*, *54*(3), 267–281, doi:10.1007/s10874-006-9026-x.

Pehkonen, S. O., et al. (1993), Photoreduction of iron oxyhydroxides in the presence of important atmospheric organic compounds, *Environ. Sci. Technol.*, *27*, 2056–2062, doi:10.1021/es00047a010.

Prahalad, A. K., et al. (2001), Air pollution particles mediated oxidative DNA base damage in a cell free system and in human airway epithelial cells in relation to particulate metal content and bioreactivity, *Chem. Res. Toxicol.*, *14*(7), 879–887, doi:10.1021/tx010022e.

Rastogi, N., et al. (2009), New technique for online measurements of water-soluble Fe(II) in atmospheric aerosols, *Environ. Sci. Technol.*, *43*(7), 2425–2430, doi:10.1021/es8031902.

Reddy, M. S., et al. (2005), Evaluation of the emission characteristics of trace metals from coal and fuel oil fired power plants and their fate during combustion, *J. Hazard. Mater.*, *123*, 242–249, doi:10.1016/j.jhazmat.2005.04.008.

Schauer, J. J. (2003), Evaluation of elemental carbon as a marker for diesel particulate matter, *J. Expo. Anal. Environ. Epidemiol.*, *13*, 443–453, doi:10.1038/sj.jea.7500298.

Sedlak, D. L., et al. (1997), The cloudwater chemistry of iron and copper at Great Dun Fell, U.K., Atmos. *Environ.*, *31*(16), 2515–2526, doi:10.1016/S1352-2310(96)00080-5.

Sedwick, P. N., et al. (2007), Impact of anthropogenic combustion emission on the fractional solubility of aerosol iron: Evidence from the Sargasso Sea, *Geochem. Geophys. Geosyst.*, *8*, Q10Q06, doi:10.1029/2007GC001586.

See, S. W., et al. (2007), Contrasting reactive oxygen species and transition metal concentrations in combustion aerosols, *Environ. Res.*, *103*(3), 317–324, doi:10.1016/j.envres.2006.08.012.

Shaked, Y., et al. (2005), A genetic kinetic model for iron acquisition by eukaryotic phytoplakton, *Limnol. Oceanogr.*, *50*(3), 872–882.

Siefert, R. L., et al. (1994), Iron photochemistry of aqueous suspensions of ambient aerosol with added organic acids, *Geochim. Cosmochim. Acta*, *58*(15), 3271–3279, doi:10.1016/0016-7037(94)90055-8.

Siefert, R. L., et al. (1999), Chemical characterization of ambient aerosol collected during the southwest monsoon and intermonsoon seasons over the Arabian Sea: Labile-Fe(II) and other trace metals, *J. Geophys. Res.*, *104*(D3), 3511–3526, doi:10.1029/1998JD100067.

Smith, R. D. (1980), The trace element chemistry of coal during combustion and the emissions from coal-fired plants, *Prog. Energy Combust. Sci.*, *6*, 53–119, doi:10.1016/0360-1285(80)90015-5.

Solmon, F., et al. (2009), Acidic processing of mineral dust iron by anthropogenic compounds over the north Pacific Ocean, *J. Geophys. Res.*, *114*, D02305, doi:10.1029/2008JD010417.

Solomon, P. A., et al. (2003), Overview of the 1999 Atlanta Supersite Project, *J. Geophys. Res.*, *108*(D7), 8413, doi:10.1029/2001JD001458.

Stookey, L. L. (1970), Ferrozine—A new spectrophotometric reagent for iron, *Anal. Chem.*, *42*(7), 779–781, doi:10.1021/ac60289a016.

Streets, D. G., et al. (2001), Black carbon emissions in China, *Atmos. Environ.*, *35*, 4281–4296, doi:10.1016/S1352-2310(01)00179-0.

Tao, F., et al. (2003), Reactive oxygen species in pulmonary inflammation by ambient particulates, *Free Radic. Biol. Med.*, *35*(4), 327–340, doi:10.1016/S0891-5849(03)00280-6.

Valavanidas, A., et al. (2000), Generation of hydroxyl radicals by urban suspended particulate air matter. The role of iron ions, *Atmos. Environ.*, *34*(15), 2379–2386, doi:10.1016/S1352-2310(99)00435-5.

Vidrio, E., et al. (2008), Generation of hydroxyl radicals from dissolved transition metals in surrogate lung fluid solutions, *Atmos. Environ.*, *42*(18), 4369–4379, doi:10.1016/j.atmosenv.2008.01.004.

Weber, R. J., et al. (2003), Short-term temporal variation in PM2.5 mass and chemical composition during the Atlanta supersite experiment, 1999, *J. Air Waste Manag. Assoc.*, *53*, 84–91.

Willey, J. D., et al. (2000), Temporal variability of iron speciation in coastal rainwater, *J. Atmos. Chem.*, *37*(2), 185–205, doi:10.1023/A:1006421624865.

Yamasoe, M., et al. (2000), Chemical composition of aerosol particles from direct emissions of vegetation fires in the Amazon Basin: Water-soluble species and trace elements, *Atmos. Environ.*, *34*(10), 1641–1653, doi:10.1016/S1352-2310(99)00329-5.

Zhang, Y. X., et al. (2008), Source apportionment of in vitro reactive oxygen species bioassay activity from atmospheric particulate matter, *Environ. Sci. Technol.*, *42*(19), 7502–7509, doi:10.1021/es800126y.

Zhu, X., et al. (1993), Photoreduction of iron(III) in marine mineral aerosol solutions, *J. Geophys. Res.*, *98*(D5), 9039–9046, doi:10.1029/93JD00202.

Zhuang, G., et al. (1992), Link between iron and sulphur cycles suggested by detection of Fe(II) in remote marine aerosols, *Nature*, *355*, 537–539, doi:10.1038/355537a0.

E. S. Edgerton, Atmospheric Research and Analysis, Inc., 410 Midenhall Way, Cary, NC 27513, USA.

B. J. Majestic, Department of Chemistry and Biochemistry, Northern Arizona University, PO Box 5698, Flagstaff, AZ 86011-5698, USA.

M. Oakes, N. Rastogi, and R. J. Weber, School of Earth and Atmospheric Sciences, Georgia Institute of Technology, 311 Ferst Dr., Atlanta, GA 30332, USA. (michelle.oakes@eas.gatech.edu)

J. J. Schauer, Department of Civil and Environmental Engineering, University of Wisconsin-Madison, 148 Water Science and Engineering Laboratory, 660 North Park St., Madison, WI 53706-1484, USA.

M. Shafer, Department of Civil and Environmental Engineering, University of Wisconsin-Madison, 201A Water Science and Engineering Laboratory, 660 North Park St., Madison, WI 53706-1484, USA.